

Numerical Study of the Effect of Anthropogenic Aerosols on Spring Persistent Rain over Eastern China

DENG Jiechun^{1,2} (邓洁淳), XU Haiming^{1,2*} (徐海明), MA Hongyun^{1,2} (马红云),
and JIANG Zhihong^{1,2} (江志红)

¹ Collaborative Innovation Center on Forecast and Evaluation of Meteorological Disasters, Nanjing University
of Information Science & Technology, Nanjing 210044

² Key Laboratory of Meteorological Disasters of Ministry of Education, Nanjing University of Information
Science & Technology, Nanjing 210044

(Received October 11, 2013; in final form March 13, 2014)

ABSTRACT

The effect of anthropogenic aerosols on the spring persistent rain (SPR) over eastern China is investigated by using a high-resolution Community Atmosphere Model version 5.1 (CAM5.1). The results show that the SPR starts later due to anthropogenic aerosols, with a shortened duration and reduced rainfall amount. A reduction in air temperature over the low latitudes in East Asia is linked to anthropogenic aerosols; so is a weakened southwesterly on the north side of the subtropical high. Meanwhile, air temperature increases significantly over the high latitudes. This north-south asymmetrical thermal effect acts to reduce the meridional temperature gradient, weakening the upper-level westerly jet over East Asia and the vertical motion over southeastern China. As a result, the SPR is reduced and has a much shorter duration. The indirect effect of anthropogenic aerosols also plays an important role in changing the SPR. Cloud droplet number concentration increases due to anthropogenic aerosols acting as cloud condensation nuclei, leading to a reduction in cloud effective radius over eastern China and a reduced precipitation efficiency there.

Key words: CAM5.1 model, anthropogenic aerosols, East Asian climate, spring persistent rain

Citation: Deng Jiechun, Xu Haiming, Ma Hongyun, et al., 2014: Numerical study of the effect of anthropogenic aerosols on spring persistent rain over eastern China. *J. Meteor. Res.*, **28**(3), 341–353, doi: 10.1007/s13351-014-3198-0.

1. Introduction

The increase in surface air temperature induced by anthropogenic black carbon (BC) is significantly greater in the Northern Hemisphere than in the Southern Hemisphere, and a northward shift of the intertropical convergence zone (ITCZ) is thus predicted (Chung and Seinfeld, 2005). However, some studies found that inter-hemispheric asymmetry cooling due to aerosols brings a significant reduction in precipitation to the north of the equator and an increase to the south, shifting the ITCZ southward (Ming and Ramaswamy, 2009; Wang et al., 2013). China, located in East Asia, is a pronounced monsoon region.

East Asian monsoons have great impacts on the regional climate change. Meanwhile, China has recently experienced a rapid economic development, and its emissions of anthropogenic aerosols have greatly increased with the expansion of urban areas along the east coast of China. These local aerosol emissions can play an important role in regional climate (Li Z. et al., 2010).

Effects of anthropogenic aerosols on East Asian monsoons have been studied and simulated. A decrease in surface temperature induced by aerosols can weaken both summer and winter monsoons (Liu et al., 2009; Deng et al., 2014a). Menon et al. (2002) showed that the solar radiation absorbed by BC could heat the

Supported by the National Basic Research and Development (973) Program of China (2010CB428505), National Natural Science Foundation of China (41275094), Priority Academic Program Development of Jiangsu Higher Education Institutions (PAPD), and Jiangsu Provincial Qinglan Project.

*Corresponding author: hxu@nuist.edu.cn.

©The Chinese Meteorological Society and Springer-Verlag Berlin Heidelberg 2014

air, leading to strengthened convective activities over southern China, which is in accordance with the “southern flood and northern drought” phenomenon in summer over China during the last 50 years. However, other studies suggested that aerosols do not contribute to the observed anomalous summer rainfall over East Asia, or even cause an opposite precipitation pattern (Gu et al., 2006; Wang et al., 2009a; Zhang H. et al., 2009; Zhang et al., 2012). Therefore, uncertainties still exist in simulating and estimating the impacts of aerosols on the summer precipitation over East Asia.

Previous studies mostly focused on East Asian summer or winter monsoons. There is a lack of research on the effect of aerosols on atmospheric circulation during spring. Tian and Yasunari (1998) advanced the concept of spring persistent rain (SPR) and regarded the SPR as a climatic event. The SPR usually occurs in the area between the middle and lower reaches of the Yangtze River and the Nanling Mountains (25° – 30° N) during March and April, which is a persistent and relatively steady pluvial period over eastern China before the onset of the South China Sea summer monsoon (SCSSM; Wan et al., 2008c). Wan et al. (2006, 2008a) suggested that the formation of the SPR was the result of mechanical forcing and thermal forcing of the Tibetan Plateau (TP) and the location and intensity of the SPR were influenced by the topography of the Nanling and Wuyi mountains. Moreover, the seasonal reverse of the zonal land-sea thermal contrast would precondition establishment of the East Asian subtropical summer monsoon (Qi et al., 2008), which may be crucial to the formation of the SPR as well (Li Chao et al., 2010; Zhang et al., 2011). Interdecadal variability of the SPR was studied by Jiang and Zhao (2012). They found a spring precipitation surplus over eastern China from the mid 1970s to the early 1980s, and a precipitation deficit after the early 1990s.

With less precipitation in the Northern Hemisphere before summer monsoon, wet deposition is at its minimum in spring, and as a result, aerosols will remain in the atmosphere for a longer time. Significant thermal responses of atmosphere to the radiative forcing of aerosols may induce changes in general cir-

ulation to influence the subsequent evolution of the East Asian summer monsoon (Lau and Kim, 2006b). Using the Community Atmosphere Model version 3.0 (CAM3.0), Wang et al. (2009b) simulated the effect of BC on summer monsoon over South Asia. They suggested that BC warmed the lower troposphere by strongly absorbing solar radiation in South Asia in late spring, leading to an advance of the rainy periods over the Bay of Bengal and its coast, together with the onset of the Indian summer monsoon. Using the same general circulation model, Hu et al. (2011) showed that the spring precipitation decreased in central to southern China but increased in northern China due to sulfate (SF) and BC over East Asia. It is noted that the response of atmosphere to the aerosols during spring is far from a simple pattern related to local direct aerosol forcing, and the structure and amplitude of such a regional response is determined by the balance of several factors, including solar heating, condensation and adiabatic heating, and turbulent diffusion in the boundary layer (Kim et al., 2006).

The purpose of this study is to investigate the impact of anthropogenic aerosols on the SPR over eastern China using a high-resolution global climate model (CAM5.1) from the National Center for Atmospheric Research (NCAR). Section 2 describes the model, experimental design, and observational data used in this study. In Section 3, the corresponding results in spring responses of atmosphere to the radiative forcing of aerosols over eastern China are presented, and a possible mechanism is discussed. Finally, the conclusions and discussion are given in Section 4.

2. Model, experimental design, and data

2.1 General circulation model and aerosol module

An earlier version of the Community Atmosphere Model (CAM3.0) has been widely used to study the effect of aerosols on the climate over East Asia (Liu et al., 2009; Wang et al., 2009a; Hu et al., 2011; Zhang et al., 2011). CAM5.1 is the latest version of the atmosphere model (Neale et al., 2010) in the Community Earth System Model version 1 (CESM1) released in

2011 by the NCAR. It could simulate the atmospheric circulation stand alone or be coupled with other models in the CESM1. Moreover, CAM5.1 provides a three-mode version of the modal aerosol module (MAM3) for long-term climate simulations, including the Aitken mode, accumulation mode, and coarse mode (Liu et al., 2012). The aerosols involved in each mode are internally mixed, which is closer to the existent state of aerosols in the observation. Therefore, the optical property of aerosols could be well described by MAM3 in CAM5.1, and the particle distribution and number concentration are accurately calculated for better simulation of the direct and indirect effects of aerosols. This aerosol module contains several main kinds of aerosols, such as SF, BC, organic carbon (OC), dust (Dst), and sea salt (SS). CAM5.1 used in this study has a high resolution of $0.9^\circ \times 1.25^\circ$ and a hybrid vertical coordinate with 30 levels, including a rigid lid at 3.643 hPa.

2.2 Experimental design

To investigate the effect of anthropogenic aerosols on the SPR over eastern China, we perform two numerical experiments, i.e., a control experiment (CTRL) with all anthropogenic aerosols forcing (for year 2000) and a sensitivity experiment (NOAERO).

In NOAERO, anthropogenic aerosols (BC, SF, and OC) linked to human activities at the surface or in the upper air over eastern China ($20^\circ\text{--}45^\circ\text{N}$, $100^\circ\text{--}125^\circ\text{E}$) are all prescribed at the pre-industrial level (for year 1850), but natural aerosols (Dst and SS) produced by natural processes such as volcanic eruptions are unadjusted (Fig. 1). The emission sources involved in both experiments are those used in the Intergovernmental Panel on Climate Change (IPCC) fifth Assessment Report (AR5) (Lamarque et al., 2010). All greenhouse gases and interactive land-atmospheric forcing are the same in both simulations. Thus, the difference between CTRL and NOAERO can be regarded as the impact of anthropogenic aerosols over eastern China on the East Asian climate.

In both experiments, sea surface temperature (SST) is prescribed with monthly mean SST from 1850 to 2010, which is a blended SST dataset with HadISST1 from the UK Met Office Hadley Center and OI SST from the National Oceanic and Atmospheric Administration (NOAA) (Hurrell et al., 2008). Consequently, the seasonal and interannual variations of the SST are present during the model integrations, and as a result the influence of the intensity of East Asian monsoons on the spatial distribution of aerosols is considered; that is, the interaction between aerosols

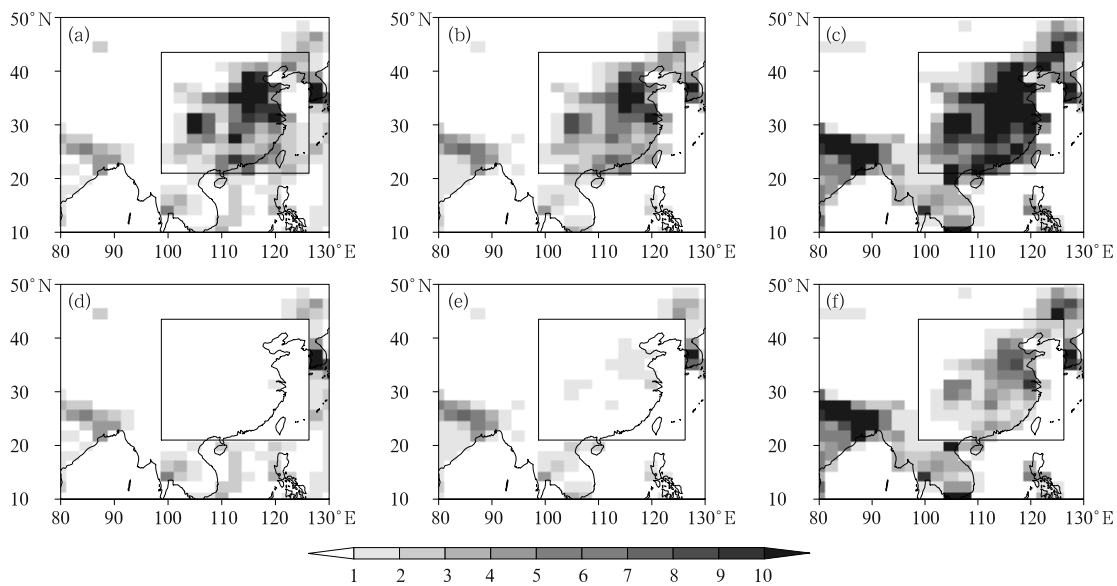


Fig. 1. Spatial distributions of initial anthropogenic aerosol emissions of (a, d) sulfate ($10^8 \text{ mol cm}^{-2} \text{ s}^{-1}$), (b, e) black carbon ($10^{10} \text{ mol cm}^{-2} \text{ s}^{-1}$), and (c, f) organic carbon ($10^{10} \text{ mol cm}^{-2} \text{ s}^{-1}$) over East Asia for (a-c) CTRL and (d-f) NOAERO.

and atmosphere is included in the experiments. Both simulations are integrated from January 1988 to December 2007, and the results from the last 15 years (1993–2007) are analyzed. Tian and Yasunari (1998) suggested that the duration of the SPR is in pentads 12–16 (March to early May), while Wan et al. (2006) noted the SPR for the period of March and April. As the pre-rainy season in South China generally occurs in mid May, the period of March to April is chosen as the SPR period in this paper as in Wan et al. (2006).

2.3 Data

The daily and monthly reanalysis from the European Centre for Medium-Range Weather Forecasts (ECMWF), namely the ERA-Interim, is used to validate the simulated atmospheric circulation. The ERA-Interim puts emphasis on improving its earlier reanalysis of ERA-40, including the representation of the hydrological cycle, the quality of the stratospheric circulation, and the consistency in time of the reanalyzed fields (Dee et al., 2011). We use the pentad precipitation dataset from the Climate Prediction Center Merged Analysis of Precipitation (CMAP; Xie and Arkin, 1997) provided by the NOAA to compare with the simulated annual cycle of precipitation over eastern China. The CMAP dataset contains precipitation distributions with a full global coverage and improved data quality compared to individual data sources (Xie and Arkin, 1997).

3. Results

3.1 Model validation

Numerous studies have simulated the features of aerosols and investigated the impacts of aerosols on regional and global climate by using CAM5.1 (Gettelman et al., 2010; Hu and Liu, 2013; Jiang et al., 2013). Liu et al. (2012) showed that CAM5.1 is able to qualitatively capture the observed geographical and temporal variation of aerosols, including aerosol mass, number concentration, size distribution, and aerosol optical properties. To examine the capability of CAM5.1 in simulating atmospheric circulation and precipitation fields over East Asia during the SPR period, Fig. 2 compares the simulated March–April mean circulation at 850 hPa and surface precipitation with observations. The simulated spatial distributions of 850-hPa wind and surface rainfall are consistent with the observations. In boreal spring, the southwesterly wind prevails over southern China (south of 30°N) with a heavy rainfall band (rainfall exceeding 3 mm day⁻¹) extending from the north side of the subtropical high over the Pacific Ocean to the east of the Philippines. There is a flow on the southeast side of the TP due to the topography, forming an approximately cyclonic circulation pattern. Meanwhile, the northwesterly wind prevails in the mid and high latitudes of East Asia, which converges with the southwesterly wind over the middle

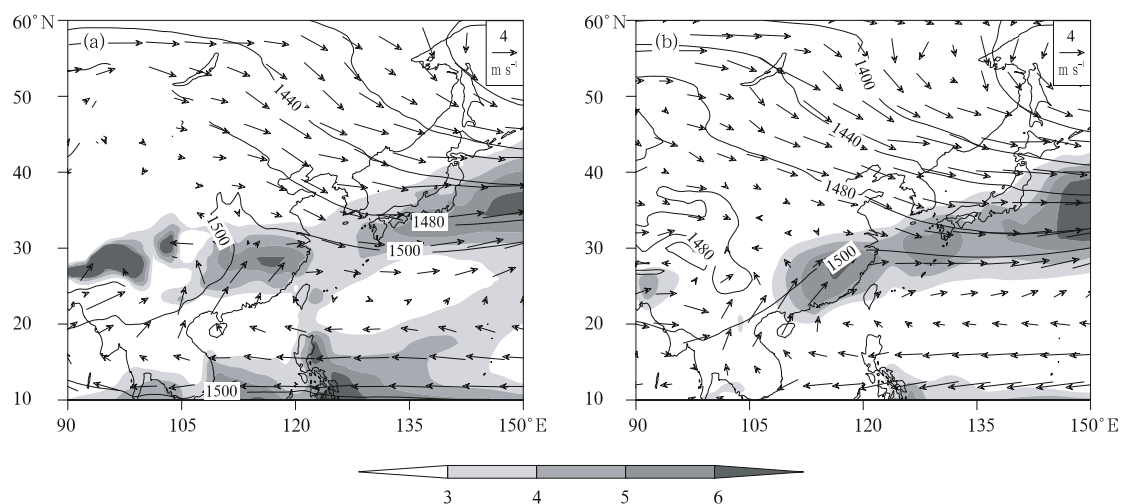


Fig. 2. March–April mean winds (vector; m s⁻¹) and geopotential height (contour; gpm) at 850 hPa and surface precipitation (shading; mm day⁻¹) from (a) CTRL and (b) observation.

and lower reaches of the Yangtze River. However, the simulated 1500-gpm isoheight at 850 hPa shifts northward in comparison with the observation, together with the SPR rain belt, leading to an underestimation of the spring rainfall over the southern coastal regions of China. Meanwhile, too much precipitation is simulated over the northwestern part of the Indo-China Peninsula and southwestern China, due to a westward shift of the subtropical high and an enhanced southwesterly in CTRL. Therefore, the spatial distribution and intensity of simulated precipitation over East Asia by CAM5.1 show some systematic errors, as seen in many other global climate models. In terms of the SPR, however, CAM5.1 still well captures the characteristics of atmospheric circulation and precipitation over eastern China.

3.2 Onset of the SPR

Figure 3 shows the latitude-time cross-section of precipitation along 110° – 122.5° E. The SPR with precipitation exceeding 4 mm day^{-1} appears in early March (pentad 15) when averaged from 1993 to 2007, and is located between 25° and 30° N over eastern China. The SPR indicates the seasonal transition of the East Asian circulation from winter to spring and the weakening of the East Asian winter monsoon system due to the shrunken land-sea thermal contrast, together with the occurrence of strong southwesterly wind and the water vapor convergence there. The rain belt remains until the end of April, but with a rel-

atively weaker and interrupted heavy rainfall center ($\geq 6 \text{ mm day}^{-1}$). The precipitation over the northern SCS exceeds 4 mm day^{-1} in pentad 26, declaring the onset of the SCSSM and the termination of the SPR. By contrast, the spring rainfall over 25° – 30° N is slightly overestimated in CAM5.1, and a northward-shifted rain belt is present in the model, which is stationary (Fig. 3b). It is clearly depicted that the spring rainfall begins in pentad 15 in CTRL with a magnitude continuously exceeding 4 mm day^{-1} , which is in coincidence with the observation.

Based on precipitation and low-level circulation, Wan et al. (2008b) defined the onset of the SPR as the first pentad after pentad 7 that satisfies the following criteria: 1) area-averaged precipitation must be greater than 4 mm day^{-1} over the SPR region (Region A: 23° – 30° N, 110° – 120° E); 2) mean southwesterly velocity at 850 hPa must be greater than 4 m s^{-1} over its upstream region (Region B: 20° – 25° N, 110° – 115° E); 3) in the subsequent three pentads, at least one pentad satisfies the above two criteria. Figure 4 shows the temporal evolutions of the aforementioned precipitation and southwesterly velocity at 850 hPa. As shown in Fig. 4a, under the influence of anthropogenic aerosols, a decrease in precipitation is obvious over Region A in pentads 14–15. Therefore, the onset time of precipitation exceeding 4 mm day^{-1} in Region A is pentad 16 in CTRL, two pentads later than that in NOAERO. Similarly, the southwesterly velocity at 850 hPa is weakened over Region B during pentads

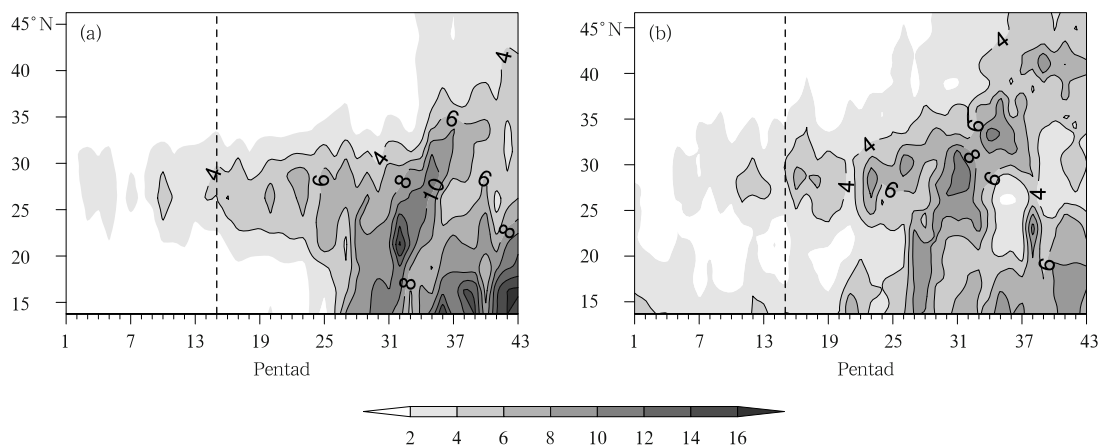


Fig. 3. Latitude-time cross-sections of precipitation along 110° – 122.5° E from (a) CMAP and (b) CTRL (shading; mm day^{-1} ; contour $\geq 4 \text{ mm day}^{-1}$).

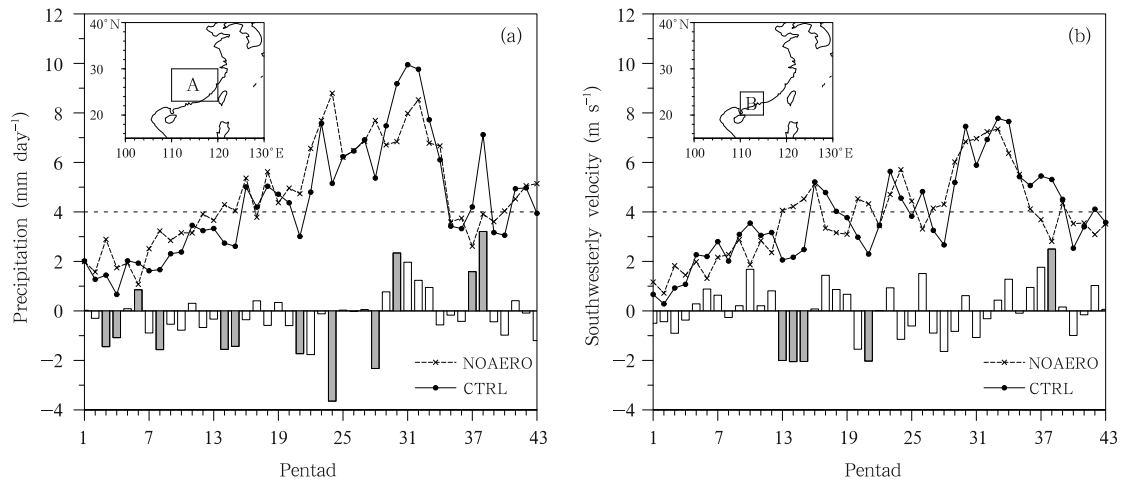


Fig. 4. Temporal evolutions of area-averaged (a) precipitation (mm day^{-1}) over the SPR region (Region A) and (b) 850-hPa southwesterly velocity (m s^{-1}) over its upstream region (Region B). Solid line is for CTRL, dashed line is for NOAERO, and bar chart is for CTRL–NOAERO. Shaded areas represent statistically significant changes at the 90% confidence level.

13–15, showing that the onset of southwesterly velocity greater than 4 m s^{-1} in CTRL is delayed by three pentads compared to that in NOAERO (Fig. 4b). As a result, the SPR is established in pentads 16 and 14 in CTRL and NOAERO, respectively, meaning a delayed onset of the SPR due to anthropogenic aerosols over eastern China. Moreover, Deng et al. (2014b) found an advanced onset of the SCSSM induced by anthropogenic aerosols using CAM5.1, indicating that the SPR is established later but also ends earlier with a shortened duration.

3.3 Precipitation and 850-hPa winds

Figure 5 shows the time series of March–April mean precipitation over Region A and 850-hPa southwesterly velocity over Region B. In most years, the SPR is reduced due to anthropogenic aerosols as a marked reduction in precipitation by 0.94 mm day^{-1} and reduced southwesterly velocity by 0.92 m s^{-1} . Figure 6a shows the mean changes of geopotential height and wind at 850 hPa in the SPR period. A positive geopotential height anomaly appears over southern China with a maximum greater than 5 gpm on the southeast side of the TP, while a negative anomaly appears over the western Pacific Ocean due to the weakening of the subtropical high. This positive and negative geopotential height anomalies form an east–west dipole pattern. Correspondingly, some anticy-

clonic anomaly flow shows up on the southeast side of the TP, which weakens the flow there. The northeasterly wind anomaly dominates southern China, the northern SCS, and the Indo-China Peninsula, while obvious northwesterly wind anomaly prevails north of the Yangtze River. Besides, there is westerly wind anomaly over the ocean east of the Philippines. As a result, the gradient of geopotential height is attenuated between the southeast side of the TP and the western Pacific Ocean under the effect of anthropogenic aerosols, leading to weakened southwesterly on the north side of the subtropical high and reduced northward transport of water vapor from the tropics. Eventually, precipitation over southern China will be suppressed associated with the circulation change. To further verify the rainfall change, Fig. 6b gives the March–April mean rainfall anomaly field. A significantly suppressed rain belt is clearly seen over southeastern China, the East China Sea, and southern Japan, and precipitation drops obviously by more than 2 mm day^{-1} over the middle and lower reaches of the Yangtze River.

3.4 Understanding the reduced SPR

Aerosols can influence the radiative balance between land and atmosphere by scattering and absorbing solar radiation and long wave radiation, which is

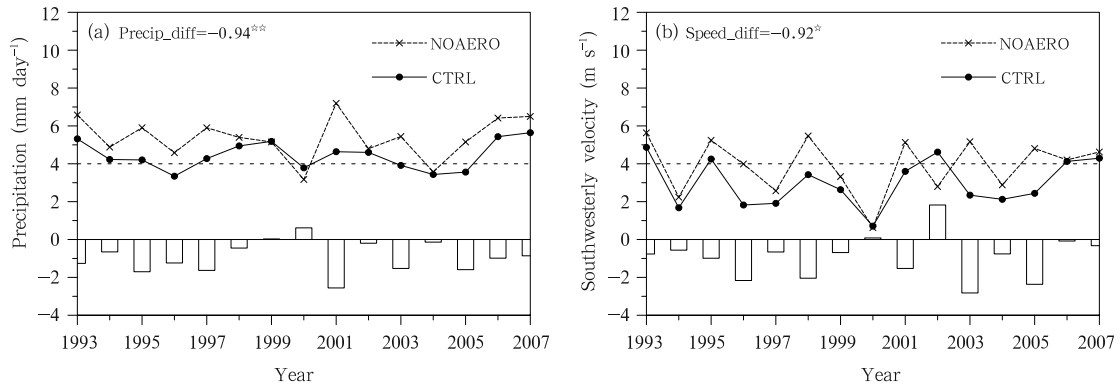


Fig. 5. Time series of March–April mean (a) precipitation (mm day^{-1}) averaged over Region A and (b) 850-hPa southwesterly velocity (m s^{-1}) averaged over Region B. Solid line is for CTRL, dashed line is for NOAERO, and bar chart is for CTRL–NOAERO. Asterisk and double-asterisk represent statistically significant changes at the 90% and 95% confidence levels, respectively.

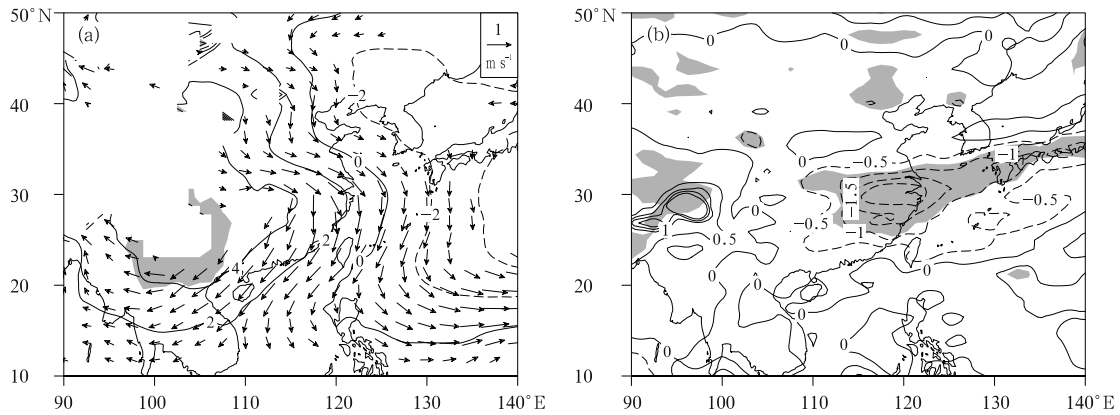


Fig. 6. March–April mean differences of (a) geopotential height and winds at 850 hPa and (b) precipitation difference between CTRL and NOAERO. Only wind changes that are significant at the 90% confidence level are plotted. Contour intervals are 2 gpm or 0.5 mm day^{-1} , with negative values given by dashed contours. Shaded areas represent statistically significant changes at the 90% confidence level.

the direct effect; so the thermal forcing of aerosols is regarded as an essential way to affecting the climate. Figure 7a shows the vertical structure of air temperature difference between CTRL and NOAERO averaged over eastern China. We can see that the air temperature decreases in the lower and upper troposphere south of 35°N with an amplitude of 0.4°C , but it increases at 200 hPa. However, anthropogenic aerosols heat the air below 250 hPa over the mid-high latitudes, with a warming amplitude greater than 1°C in the mid-lower troposphere. Accordingly, the meridional temperature gradient averaged between 850 and 200 hPa is significantly reduced over southern China, but enhanced over the region $30^\circ\text{--}50^\circ\text{N}$ (solid line in

Fig. 7b). Therefore, this north–south asymmetrical thermal effect reduces the mean meridional temperature gradient in spring over East Asia. The thermal wind relationship is as follows:

$$u_T = -\frac{R}{f} \ln \frac{p_0}{p_1} \left(\frac{\partial \bar{T}}{\partial y} \right)_p,$$

where u_T is the zonal component of thermal wind, p_0 and p_1 are pressures in the lower and upper troposphere, respectively, and $\left(\frac{\partial \bar{T}}{\partial y} \right)_p$ is the meridional temperature gradient averaged between the lower and upper troposphere. It is clear that zonal wind in the upper troposphere changes with the meridional temp-

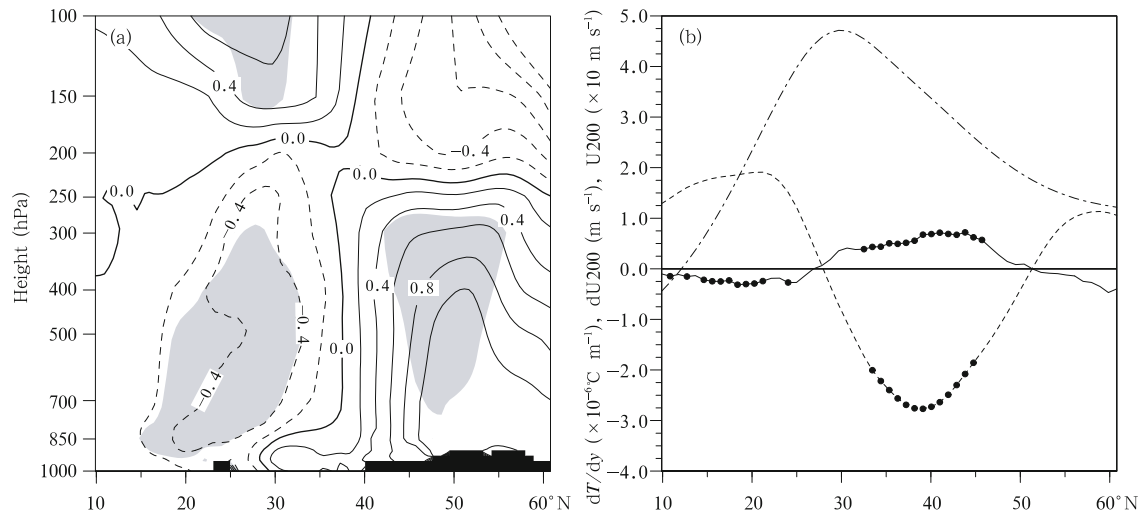


Fig. 7. (a) Vertical cross-section of temperature differences ($^{\circ}\text{C}$) between CTRL and NOAERO along 110° – 122.5°E , averaged for March and April and (b) March–April mean meridional tropospheric (850–200 hPa) temperature gradient differences (solid line; $10^{-6} \text{ }^{\circ}\text{C m}^{-1}$) and zonal wind differences (dashed line; m s^{-1}) between CTRL and NOAERO along 110° – 122.5°E , together with climatological mean zonal wind in NOAERO (dash-dotted line; 10 m s^{-1}). Shaded areas and black dots represent statistically significant changes at the 90% confidence level.

erature gradient, meaning that reduced (enhanced) meridional temperature gradient results in strengthened (weakened) westerly wind in the upper troposphere. As shown in Fig. 7b, the axis of the subtropical westerly jet (dash-dotted line) is located near 30°N in NOAERO. In CTRL, zonal wind (dashed line) is enhanced south of 30°N and weakened within 30° – 50°N with a minimum near 40°N , suggesting that the westerly jet is weaker and moves southward. Therefore, the circulation change in the upper troposphere is indeed the thermal response of atmosphere to anthropogenic aerosols, associated with the out-of-phase relationship between upper-layer zonal wind and meridional temperature gradient between the upper and lower troposphere. Meanwhile, air mass is accumulated over southern China due to aerosols' cooling effect, which explains the increase in 850-hPa geopotential height and northeasterly wind anomaly there (Fig. 6a). Eventually, the southwesterly on the north side of the subtropical high is weakened. Besides, 500-hPa geopotential height decreases over the western equatorial Pacific Ocean, the SCS, and the East Asian Continent, yielding a southward displacement of the weaker subtropical high (figure omitted). Zhang Jie et al.

(2009) suggested that the main moisture of the SPR comes from the western equatorial Pacific Ocean and both the subtropical high and the upper-level westerly jet move northward to their normal positions. Thus, after considering the effect of anthropogenic aerosols, circulation change provides adverse conditions for the maintenance of the SPR.

To further reveal the relationship between circulation change and precipitation anomaly, Fig. 8 shows the differences of wind divergence and vertical meridional circulation. Because of the weakened southwesterly over southern China (Fig. 6a), a positive divergence anomaly (solid line in Fig. 8a) occurs at 850 hPa over 25° – 35°N . Meanwhile, a significant negative anomaly (dashed line in Fig. 8a) is found in the upper troposphere south of the Yangtze River due to the weaker and southward-shifted upper-level westerly jet. Both divergence anomaly centers in the lower and upper troposphere are near the axis of the westerly jet (30°N). This aerosol-induced circulation results in a significant anomalous downward motion over southern China through weakening the pumping below the axis of the westerly jet (Fig. 8b), acting to suppress the spring precipitation there. However, the fact that

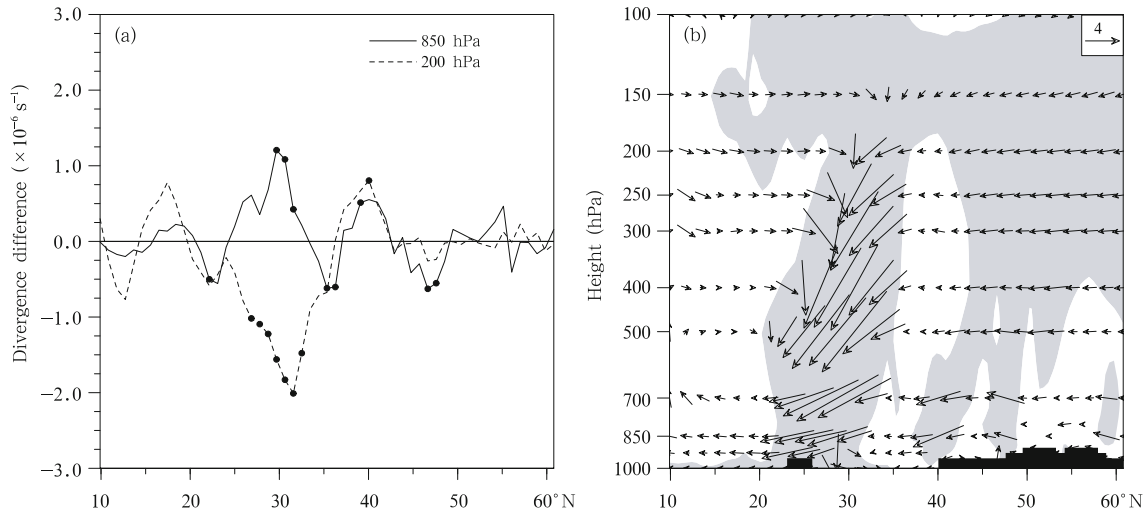


Fig. 8. March–April mean (a) divergence differences (10^{-6} s^{-1}) at 850 hPa (solid line) and 200 hPa (dashed line) and (b) meridional circulation differences (vectors; meridional wind in m s^{-1} ; vertical pressure velocity in 0.2 hPa s^{-1}) between CTRL and NOAERO along 110° – 122.5° E. Shaded areas and black dots represent statistically significant changes at the 90% confidence level.

the condensation latent heating decreases due to a weaker upward motion (figure omitted) will further decrease the meridional temperature gradient by cooling the air in the low latitudes, forming a positive feedback mechanism. Therefore, the response of air temperature to anthropogenic aerosols is determined by the radiative forcing of the aerosols and the positive feedback involved, and the thermal effect of anthropogenic aerosols is very likely to cause a primary perturbation for the adjustments of air temperature and circulation.

In addition, aerosols can serve as cloud condensation nuclei (CCN), and thus change the cloud droplet effective radius (R_{eff}), giving rise to higher cloud albedo (Twomey, 1997) and reducing precipitation efficiency due to longer cloud lifetime (Albrecht, 1989). This is the so-called indirect effect. Numerous studies have verified the impact of anthropogenic aerosols on the micro-properties of clouds through in-cloud droplet number concentration (CDNC) (Han et al., 1994; Wetzal and Stowe, 1999; Pwlowaska and Brenguier, 2000; Bréon et al., 2002). After considering the effect of anthropogenic aerosols, the aerosol optical depth increases markedly by 0.09 over the SPR region, together with CCN at supersaturation of 0.1% ($\text{CCN}_{0.1}$) by 219.9 cm^{-3} at 850 hPa (158.1%; Table

1). Figure 9 shows the changes of CDNC and R_{eff} at 850 hPa. With the increase in $\text{CCN}_{0.1}$ induced by anthropogenic aerosols, CDNC rises in southern China (Fig. 9a), especially in the SPR region by a ratio of 48.6%. The reduction of R_{eff} is clear in the SPR region (-13.5%) (Fig. 9b and Table 1), suppressing the coalescence of the cloud droplets and precipitation there. As a result, the indirect effect of anthropogenic aerosols plays an important role in reducing the SPR. However, it is noted that the impact of aerosols on precipitation is a complex matter, and it is difficult to

Table 1. March–April mean absolute and percentage changes of aerosol optical depth (AOD) at 550-nm wavelength, cloud condensation nuclei number concentration at supersaturation of 0.1% ($\text{CCN}_{0.1}$), in-cloud droplet number concentration (CDNC), and cloud droplet effective radius (R_{eff}) at 850 hPa due to anthropogenic aerosols averaged over the SPR region

Parameter	March–April mean (absolute change)
AOD	0.09 (51.1%)
$\text{CCN}_{0.1}$ (cm^{-3})	219.9 (158.1%)
CDNC (cm^{-3})	38.5 (48.6%)
R_{eff} (μm)	<i>-0.5</i> (-13.5%)

Note: *Italic* and **bold** fonts represent values statistically significant at the 95% and 99% confidence levels, respectively.

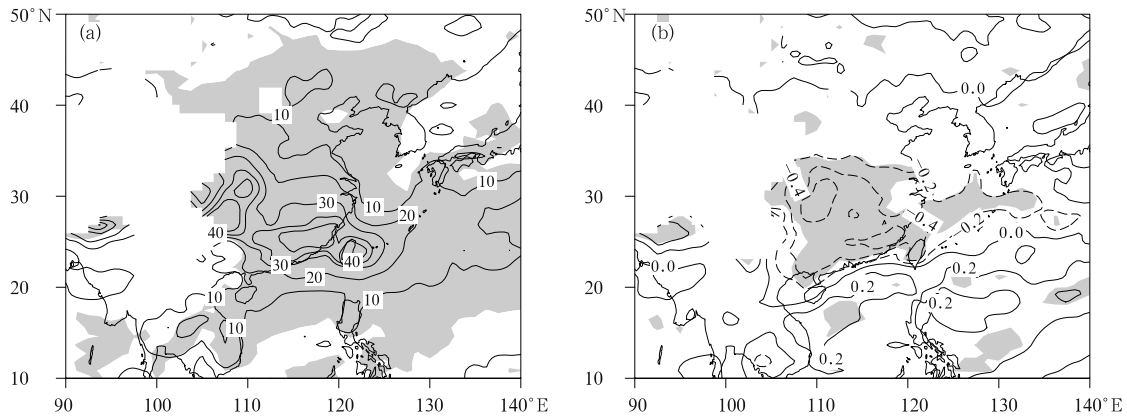


Fig. 9. March–April mean changes of (a) cloud droplet number concentration and (b) cloud droplet effective radius at 850 hPa (CTRL minus NOAERO). Contour intervals are 10 cm^{-3} and $0.2 \mu\text{m}$, respectively, with negative values given by dashed contours. Shaded areas represent statistically significant changes at the 90% confidence level.

find the exact relationship between CCN and rainfall. Nonlinearity between in-cloud microphysical parameters and surface rainfall remains uncertain. Furthermore, the cloud-aerosol interaction is also influenced by the background circulation, such as atmospheric stability and wind shear (Yang et al., 2011).

In general, the thermal forcing associated with anthropogenic aerosols induces circulation changes over East Asia. On the other hand, the indirect effect of anthropogenic aerosols has a great impact on clouds in southern China. Both effects of the aerosol forcing suppress the SPR, which could be summarized as follows. Under the impact of anthropogenic aerosols, the decrease in air temperature leads to increased 850-hPa geopotential height in the low latitudes over East Asia, reducing the geopotential gradient between the south side of the TP and the western Pacific Ocean and weakening the southwesterly on the north side of the subtropical high in the lower troposphere, together with convergence in southern China. In comparison, a marked increase in air temperature is found in the mid-high latitudes, which reduces the meridional temperature gradient between the upper and lower troposphere. The upper-level westerly jet is weaker and shifts southward, giving rise to reduced convergence in the upper troposphere. This anomalous circulation leads to weakened upward motion and suppressed spring rainfall with a shortened duration. Moreover, in the SPR region, 850-hPa CDNC increases due to anthropogenic aerosols acting as CCN, leading to a

decrease in R_{eff} . As a result, the SPR is also suppressed by reduced coalescence of cloud droplets.

Hu and Liu (2013) noted that anthropogenic aerosols affected the decadal change of late spring precipitation in South China during 1950–2000. The mechanism of aerosols affecting spring rainfall by adjustment of circulation in East Asia is in coincidence with our results. Therefore, our results confirm the crucial role of anthropogenic aerosols in spring climate change in East Asia. However, the SPR usually occurs in early spring (March–mid April), with pre-rainy season in southern China in late spring (late April–May). Although both rainfall periods are considered spring precipitation in southern China, the features of precipitation and the intensity of circulation are different for these periods. Thus, further studies are needed to investigate the effect of anthropogenic aerosols during different spring precipitation periods.

4. Conclusions and discussion

Based on a high-resolution model of CAM5.1, the impact of anthropogenic aerosols on the SPR over eastern China is investigated in this study. The results are as follows.

(1) The SPR is established two pentads later due to anthropogenic aerosols, together with a shortened duration and reduced precipitation amount.

(2) Under the influence of anthropogenic aerosols, a significant decrease in air temperature leads to an

increase in 850-hPa geopotential height in the low latitudes over East Asia, reducing the geopotential gradient between the south side of the TP and the western Pacific Ocean and weakening the southwesterly on the north side of the subtropical high in the lower troposphere, together with convergence over southern China. In comparison, a marked increase in air temperature is found in the mid-high latitudes. This north-south asymmetrical thermal effect acts to reduce the meridional temperature gradient so the upper-level westerly jet is weaker and shifts southward, giving rise to reduced convergence in the upper troposphere. As a result, the SPR is suppressed with a shortened duration.

(3) The indirect effect of anthropogenic aerosols also plays an important role in reducing the SPR. CDNC in the lower troposphere is increased by aerosols acting as CCN in the SPR region, leading to an evident decrease in R_{eff} . As a result, the SPR is further suppressed due to reduced coalescence of cloud droplets.

In this study, we only explored the effect of anthropogenic aerosols on the SPR over eastern China, though remote aerosols could also enhance the impact of local aerosols in the monsoon region (Cowan and Cai, 2011). Furthermore, because of the SST response to aerosol forcing, the influence of aerosols on precipitation presented in the air-sea coupled model differs from that in the atmosphere model driven by prescribed SST (Chung et al., 2002; Wang et al., 2005; Lau and Kim, 2006a). Our future studies will use a fully coupled model including the SST response to aerosol forcing to better understand the impact of anthropogenic aerosols on spring climate in East Asia.

Acknowledgments. We thank three anonymous reviewers for their valuable comments and suggestions. Thanks also go to Dr. Zuojun Yu for her careful review of the language and kindly help in improving the English.

REFERENCES

- Albrecht, B. A., 1989: Aerosols, cloud microphysics, and fractional cloudiness. *Science*, **245**, 1227–1230.
- Bréon, F. M., D. Tanré, and S. Generoso, 2002: Aerosol effect on cloud droplet size monitored from satellite. *Science*, **295**, 834–838.
- Chung, C. E., S. Nigam, and J. T. Kiehl, 2002: Effects of the South Asian absorbing haze on the northeast monsoon and surface–air heat exchange. *J. Climate*, **15**, 2462–2476.
- Chung, S. H., and J. H. Seinfeld, 2005: Climate response of direct radiative forcing of anthropogenic black carbon. *J. Geophys. Res.*, **110**, D11102, doi: 10.1029/2004JD005441.
- Cowan, T., and W. Cai, 2011: The impact of Asian and non-Asian anthropogenic aerosols on the 20th century Asian summer monsoon. *Geophys. Res. Lett.*, **38**, L11703, doi: 10.1029/2011GL047268.
- Dee, D. P., S. M. Uppala, A. J. Simmons, et al., 2011: The ERA-Interim reanalysis: Configuration and performance of the data assimilation system. *Quart. J. Roy. Meteor. Soc.*, **137**, 553–597.
- Deng Jiechun, Xu Haiming, Ma Hongyun, et al., 2014a: The effects of anthropogenic aerosols over eastern China on East Asian monsoons in a high resolution CAM5.1 model. *J. Trop. Meteor.*, **30**, in press. (in Chinese)
- , —, —, et al., 2014b: A numerical study of the effect of anthropogenic aerosols over eastern China on East Asian summer monsoon onset and its northward advancement. *J. Trop. Meteor.*, **30**, in press. (in Chinese)
- Gettelman, A., X. Liu, S. J. Ghan, et al., 2010: Global simulations of ice nucleation and ice supersaturation with an improved cloud scheme in the Community Atmosphere Model. *J. Geophys. Res.*, **115**, D18126, doi: 10.1029/2009JD013797.
- Gu, Y., K. N. Liou, Y. Xue, et al., 2006: Climatic effects of different aerosol types in China simulated by the University of California, Los Angeles atmospheric general circulation model. *J. Geophys. Res.*, **111**, doi: 10.1029/2005JD006312.
- Han, Q., W. B. Rossow, and A. A. Lacis, 1994: Near-global survey of effective cloud droplet radii in liquid water clouds using ISCCP data. *J. Climate*, **7**, 465–497.
- Hu Haibo, Liu Chao, Zhang Yuan, et al., 2011: The effects of aerosols in CAM3.0 on climate in East Asia during boreal spring. *Scientia Meteor. Sinica*, **31**, 466–474. (in Chinese)
- Hu, N., and X. Liu, 2013: Modeling study of the effect of anthropogenic aerosols on late spring drought in South China. *Acta Meteor. Sinica*, **27**, 701–715.

- Hurrell, J. W., J. J. Hack, D. Shea, et al., 2008: A new sea surface temperature and sea ice boundary dataset for the Community Atmosphere Model. *J. Climate*, **21**, 5145–5153.
- Jiang Pinping and Zhao Ping, 2012: The interannual variability of spring rainy belt over southern China and the associated atmospheric circulation anomalies. *Acta Meteor. Sinica*, **70**, 681–689. (in Chinese)
- Jiang, Y., X. Liu, X. Q. Yang, et al., 2013: A numerical study of the effect of different aerosol types on East Asian summer clouds and precipitation. *Atmos. Environ.*, **70**, 51–63.
- Kim, M. K., K. M. Lau, M. Chin, et al., 2006: Atmospheric teleconnection over Eurasia induced by aerosol radiative forcing during boreal spring. *J. Climate*, **19**, 4700–4718.
- Lamarque, J. F., T. C. Bond, V. Eyring, et al., 2010: Historical (1850–2000) gridded anthropogenic and biomass burning emissions of reactive gases and aerosols: Methodology and application. *Atmos. Chem. Phys.*, **10**, 7017–7039.
- Lau, K. M., and K. M. Kim, 2006a: Observational relationships between aerosol and Asian monsoon rainfall, and circulation. *Geophys. Res. Lett.*, **33**, L21810, doi: 10.1029/2006GL027546.
- , M. K. Kim, and K. M. Kim, 2006b: Asian summer monsoon anomalies induced by aerosol direct forcing: The role of the Tibetan Plateau. *Climate Dyn.*, **26**, 855–864.
- Li Chao, Xu Haiming, Zhu Suxing, et al., 2010: Numerical analysis on formation mechanism of spring persistent rain. *Plateau Meteor.*, **29**, 99–108. (in Chinese)
- Li, Z., K. Lee, Y. Wang, et al., 2010: First observation-based estimates of cloud-free aerosol radiative forcing across China. *J. Geophys. Res.*, **115**, doi: 10.1029/2009JD013306.
- Liu, X., R. C. Easter, S. J. Ghan, et al., 2012: Toward a minimal representation of aerosols in climate models: Description and evaluation in the Community Atmosphere Model CAM5. *Geosci. Model Dev.*, **5**, 709–739.
- Liu, Y., J. Sun, and B. Yang, 2009: The effects of black carbon and sulfate aerosols in China regions on East Asian monsoons. *Tellus(B)*, **61**, 642–656.
- Menon, S., J. Hansen, L. Nazarenko, et al., 2002: Climate effects of black carbon aerosols in China and India. *Science*, **297**, 2250–2253.
- Ming, Y., and V. Ramaswamy, 2009: Nonlinear climate and hydrological response to aerosol effects. *J. Climate*, **22**, 1329–1339.
- Neale, R. B., A. Gettelman, S. Park, et al., 2010: Description of the NCAR Community Atmosphere Model (CAM5.0). NCAR Technical Note NCAR/TN-486+STR: 7–8.
- Pwlowaska, H., and J. L. Brenguier, 2000: Microphysical properties of stratocumulus clouds during ACE-2. *Tellus*, **52B**, 868–887.
- Qi, L., J. He, Z. Zhang, et al., 2008: Seasonal cycle of the zonal land-sea thermal contrast and East Asian subtropical monsoon circulation. *Chinese Sci. Bull.*, **53**, 131–136.
- Tian, S. F., and T. Yasunari, 1998: Climatological aspects and mechanism of spring persistent rains over central China. *J. Meteor. Soc. Japan*, **76**, 57–71.
- Twomey, S., 1997: The influence of pollution on the short-wave albedo of clouds. *J. Atmos. Sci.*, **34**, 1149–1152.
- Wan Rijin and Wu Guoxiong, 2006: Mechanism of the spring persistent rains over southeastern China. *Sci. China (Earth Science)*, **50**, 130–144. (in Chinese)
- and —, 2008a: Temporal and spatial distribution of the spring persistent rains over southeastern China. *Acta Meteor. Sinica*, **66**, 310–319. (in Chinese)
- , Wang Tongmei, and Wu Guoxiong, 2008b: Temporal variations of the spring persistent rains and SCS subtropical high and their correlations to the circulation and precipitation of the East Asian summer monsoon. *Acta Meteor. Sinica*, **66**, 800–807. (in Chinese)
- , Zhao Bingke, and Hou Yiling, 2008c: Interannual variability of spring persistent rain over southeastern China and its effect factor. *Plateau Meteor.*, **27**, 118–123. (in Chinese)
- Wang, B., Q. Ding, X. Fu, et al., 2005: Fundamental challenge in simulation and prediction of summer monsoon rainfall. *Geophys. Res. Lett.*, **32**, L15711, doi: 10.1029/2005GL022734.
- Wang, Z., H. Zhang, J. N. Li, et al., 2013: Radiative forcing and climate response due to the presence of black carbon in cloud droplets. *J. Geophys. Res.*, **118**, 3662–3675.
- Wang Zhili, Guo Pinwen, and Zhang Hua, 2009a: A numerical study of direct radiative forcing due to black carbon and its effects on the summer precipitation in China. *Climatic Environ. Res.*, **14**, 161–171. (in Chinese)

- , Zhang Hua, and Guo Pinwen, 2009b: Effects of black carbon aerosol in South Asia on Asian summer monsoon. *Plateau Meteor.*, **28**, 419–424. (in Chinese)
- Wetzel, M. A., and L. L. Stowe, 1999: Satellite-observed patterns in stratus microphysics, aerosol optical thickness, and shortwave radiative forcing. *J. Geophys. Res.*, **104**, 31287–31299, doi: 10.11029/1999JD900922.
- Xie, P., and P. A. Arkin, 1997: Global precipitation: A 17-year monthly analysis based on gauge observations, satellite estimates, and numerical model outputs. *Bull. Amer. Meteor. Soc.*, **78**, 2539–2558.
- Yang Huiling, Xiao Hui, and Hong Yanchao, 2011: Progress in impacts of aerosol on cloud properties and precipitation. *Climatic Environ. Res.*, **16**, 525–542. (in Chinese)
- Zhang Bo, Zhong Shanshan, Zhao Bin, et al., 2011: The influence of the subtropical sea surface temperature over the western Pacific Ocean on spring persistent rains. *J. Appl. Meteor. Sci.*, **22**, 57–65. (in Chinese)
- Zhang, H., Z. Wang, P. Guo, et al., 2009: A modeling study of the effects of direct radiative forcing due to carbonaceous aerosol on the climate in East Asia. *Adv. Atmos. Sci.*, **26**, 1–10.
- , —, Z. Wang, et al., 2012: Simulation of direct radiative forcing of aerosols and their effects on East Asian climate using an interactive AGCM-aerosol coupled system. *Climate Dyn.*, **38**, 1675–1693.
- Zhang Jie, Zhou Tianjun, Yu Rucong, et al., 2009: Atmospheric water vapor transport and corresponding typical anomalous spring rainfall patterns in China. *Chinese J. Atmos. Sci.*, **33**, 121–134. (in Chinese)